International Journal of Thermal Technologies
E-ISSN 2277 – 4114

Available at http://inpressco.com/category/ijtt/

Research Article

Numerical Analysis of Induction Heating of Wire

Ishant Jain[Å*], J K Saha[Å] and S. K. Ajmani[Å]

[Å]Research and Development, Tata Steel, Jamshedpur – 831007, India

Accepted 29 May 2014, Available online 01 June 2014, **Vol.4, No.2 (June 2014)**

Abstract

In the present work a numerical study was carried out to study the induction heating phenomena in a wire moving inside a long tunnel furnace. A mathematical model based on the heat transfer was developed in 'C' programming. The skin effect of the induction heating phenomenon over the periphery of the cylindrical wire was considered and applied in the form of a heat source boundary condition at the surface and inside the wire. Plant trial was conducted using a 60 KW wire heating induction furnace and the complete setup of the induction heating of moving wire was replicated. Four successful plant trials were conducted for Φ3.5 mm wire with different wire speed. Tensile testing of the specimen was performed to ascertain the desired temperature range between the center and the surface. The model predicted temperature profile obtained for different line speed of the wire was validated against the trial data and a close agreement between the model and the trial temperature profiles was found.

Keywords: *Wire, Induction heating, Skin effect, Modelling, wire heating, finite difference method*

1. Introduction

Induction heating is increasingly used in the last few decades in various industrial manufacturing processes. It can be used at low frequencies (~50 Hz) for initial preheating of wire before drawing and at higher frequencies (~ 4KHz -10 KHz) for processes involving metallurgical heat treatment (Davies, 1990) (D. R. Poirier, 2012). The main advantages include fast heating rate, great precision in heating localization, instantaneous start/ stop and good reproducibility (Davies, 1990).

The induction heating of wire at wire mill is done for the sole purpose to provide the moving wire at the hot working stage with the desired (typically uniform) temperature across its diameter.

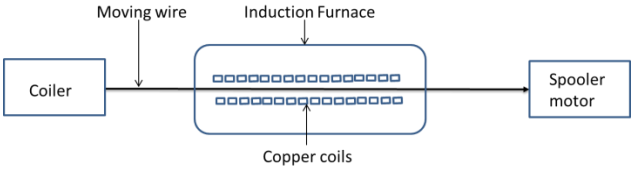

Figure 1 Schematic of Induction heating of wire at wire mill

Figure 1 shows schematic of the line heating of wire. The progressive multistage heating mode of induction heating is used where the workpiece (or wire) is moved via an indexing mechanism through a multi coil heating furnace (Edgar Rapoport, 2010). The wire coming from the coiler is made to pass through the furnace where the forward moving force is provided by the spooler motor as shown in Figure 1. The main challenge arises from the necessity to provide a uniform core to surface temperature. It is due to the skin effect that the surface is heated much faster (Edgar Rapoport, 2010)

For the current work, basic induction setup for the tunnel furnace was used. It consists of two coils with 24 turns each, for preheating and constant heating purpose, and wire as a continuous metal work piece. The work piece is secondary while the surrounding copper coil is the primary, linked or coupled with air, forming an air core transformer as shown in Figure 2. The coils are supplied with an alternating current with a frequency range of 4KHz - 5KHz, inducing a rapid oscillating magnetic field which in turn induces eddy currents over the periphery of the wire due to skin effect on account of the Joule effect. The cooling of the induction coils is provided by allowing water to flow through the cooling channels embedded inside the coils. The total heat loss enables to calculate the efficiency of the furnace.

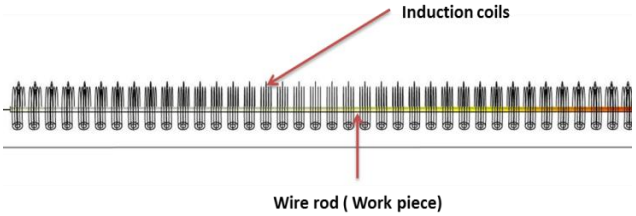

Figure 2 Induction heating of a wire

The problem was conceptualized as a basic industrial heating operation by heat transfer, reducing the complexity of coupling the Maxwell's equation with the Heat transfer equation. A mathematical model was developed based on the finite difference method to study

*Corresponding author: Mob: +918092086073, Phone: +916572248924

the thermal profile within the wire. The residence time of the wire was calculated for different line speed and variation of thermal profile was analyzed. Separate equation was developed for the power consumption inside the wire as a function of radius which was used as a boundary condition. This unique boundary condition was applied to compensate the skin effect in induction heating phenomena.

The analysis was done for Φ 3.5 mm wire, considering simple heating of a stationary cylindrical wire heated for a particular line speed. Initially the model was developed for uniform grid width where it had predicted a much lower value than the experimentally obtained values. The inaccuracy was due to very sharp change in the magnitude of the source term 'S' in the penetration depth zone called as skin depth. Hence, tuning of the model was done with variable grid size in geometric progression.

Plant trials were conducted with an in-house developed wire heating setup. An arrangement was made so that the line speed of the continuous moving wire inside the furnace can be varied. A series of experiments were conducted for various line speeds. The surface temperature of the wire was measured immediately after the exit of the furnace using the surface temperature probe. Tensile testing was performed in the laboratory for the heat treated wire samples to ascertain whether the desired temperature profile was achieved based on the percentage uniform elongation.

2. Model development

Mathematical model of a stationary wire in FDM

The governing heat transfer equation in cylindrical coordinates (D. R. Poirier, 2012) is given as::

Equation 1

$$\frac{1}{r}\frac{\partial}{\partial r}(\mathrm{K}\, r\frac{\partial T}{\partial r})+\frac{1}{r^2}\frac{\partial}{\partial \theta}(\mathrm{K}\frac{\partial T}{\partial \theta})+\frac{\partial}{\partial z}(\mathrm{K}\frac{\partial T}{\partial z})+S=\rho C_p\frac{\partial T}{\partial t}$$

The equation 1 allows essentially three-dimensional nonuniform distribution of internal source (S) caused by an electromagnetic field generated by induction coil, which result in temperature distribution within the wire. The mathematical model is based on the assumption of neglecting the heat flow in the circumferential direction because of symmetry. Heat transfer in the axial direction was ignored considering L >> D, where L is the length of wire inside the furnace and D id diameter of the wire.

The heat transfer on account of bulk motion was ignored because the value of Peclet number was considerably high i.e. P_e < 100. Peclet number was calculated using the formula

$$P_e=\frac{advection\,of\ flow}{rate\,of\ diffusion}=\frac{V\rho C_p D}{K}$$

Where V is the line speed in m/s, ρ is the density in kg/m^3, D is the diameter of the wire (m), C_p is the specific heat capacity in J/KgK and K is the thermal conductivity in W/mK. The final governing equation for heat transfer assuming constant thermal conductivity in cylindrical coordinates is given by equation 2.

Equation 2

$$\frac{1}{r}\frac{\partial}{\partial r}(r\frac{\partial T}{\partial r})+\frac{S}{K}=\frac{1}{\alpha}\frac{\partial T}{\partial t}$$

Equation 2 was discretized using finite difference method. The cross section of the wire is divided into a number of concentric rings (say m) of variable width, with the center at m=0 and the outer surface was denoted as m=M as shown in the Figure 3.

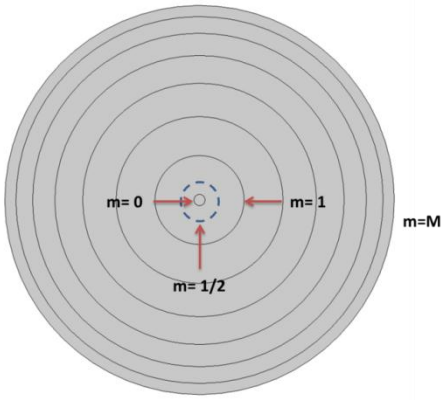

Figure 3 Concentric ring with variable width spacing between nodes

The variable width between the consecutive concentric rings was taken in geometric progression (GP) to account for the sharp change in the magnitude of the source term 'Q' into the penetration depth zone i.e. the skin depth.

The finite difference equation for the nodes :

The FD equation for any internal node 'm'

The cell width between m=0 and m=1 is denoted by Δr and is taken according to a geometric progression. Hence, the cell width between the two nodes m-1 and m is Δr_m = Δr x r $^{m-1}$ as shown in Figure 4, where r is the common ratio. It is to be noted that the derived equation can be used for constant cell width by taking the common factor of the GP as unity.

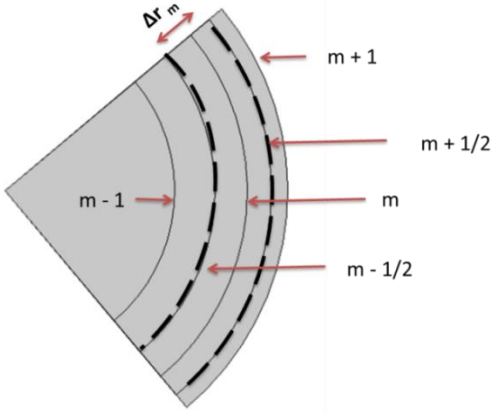

Figure 4 Schematic of an internal node m

Now, for a **node with m = -1/2** shown as a dotted line in Figure 4, the FD equation can be written as

Equation 3

$$\frac{\partial T}{\partial r}|_{m-1/2}=\frac{T_m-T_{m-1}}{\Delta r_m}=\frac{T_m-T_{m-1}}{\Delta r\times r^{m-1}},$$

And at **node m +1/2,** the FD equation is

Equation 4

$$\frac{\partial T}{\partial r}|_{m+1/2}=\frac{T_{m+1}-T_m}{\Delta r\times r^{m}}$$

For the node m as shown in Figure 4 above, the equation can be written as:

$$\frac{\partial^2 T}{\partial r^2}|_m=\frac{\frac{\partial T}{\partial r}|_{m+1/2}-\frac{\partial T}{\partial r}|_{m-1/2}}{\frac{\Delta r\times r^m}{2}+\frac{\Delta r\times r^{m-1}}{2}}=\frac{T_{m+1}-T_m-r(T_m-T_{m-1})}{\frac{1}{2}r(\Delta r\times r^{m-1})^2(1+r)}$$

Equation 5

$$\frac{\partial T}{\partial r}|_m=\frac{T_{m+1}-T_{m-1}}{\Delta r\times r^{m-1}(1+r)}$$

Substituting eq^n 3, 4 and 5 into equation 2:

Equation 6

$$T_m^{i+1}=\frac{\alpha\Delta t}{\Delta r^2 r^{m-1}(m+1)}(\frac{2}{r^{m-1}}-\frac{r-1}{r^m-1})T_{m-1}^i+(1-\frac{2\alpha\Delta t}{\Delta r^2 r^{2m-1}})T_m^i$$
$$+\frac{\alpha\Delta t}{\Delta r^2 r^{m-1}(r+1)}(\frac{r-1}{r^m-1}+\frac{2}{r^m})T_{m+1}^i+\frac{\alpha\Delta t}{k}S$$

FD equation for any center, m=0

Rate of accumulation of heat at the surface is,

$$q'=-k\times\frac{T_1^i-T_0^i}{\Delta r}$$

Therefore the rate of accumulation of heat in the portion between m=0 and m=1/2 at any instant i and per unit length is

$$q'=\{0-(k\times\frac{T_1^i-T_0^i}{\Delta r})\}\times 2\times pi\times\frac{\Delta r}{2}\times 1+S\times v$$
$$q'=k\times pi\times(T_1^i-T_0^i)\}+S\times v$$

Where v is the relevant volume, given as

$$v=pi\times(\frac{\Delta r}{r})^2\times 1$$

From the above equation, applying the energy balance,

$$q'=k\times(T_1^i-T_0^i)+S\times v=\frac{pi}{4}\times(\Delta r)^2\times\rho c_p(\frac{T_1^{i+1}-T_0^i}{\Delta t})$$

And the FD equation at m= 0 is

Equation 7

$$T_0^{i+1}=\{1-\frac{4\alpha\Delta t}{\Delta r^2}\}T_0^i+\frac{4\alpha\Delta t}{\Delta r^2}T_1^i+\frac{\alpha\Delta t}{k}S$$

FD equation on the surface, m=M,

Considering the rate of heat loss from the surface at node M, as shown in Figure 5, of the wire is q' with 'h' as the heat transfer coefficient and T_f, the outside furnace temperature.

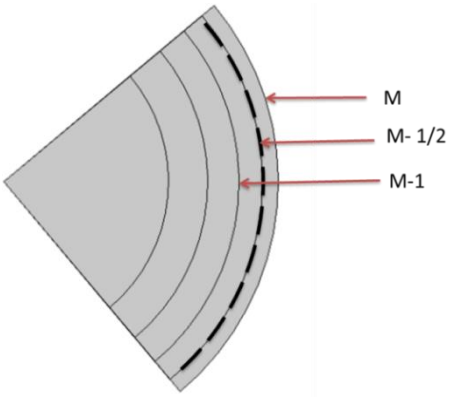

Figure 5 Schematic for the surface node M

The rate of conduction of heat between the cylindrical surface and node M-1/2 is:

$$q'=-k\times\frac{(T_M^i-T_{M-1}^i)}{\Delta r\times r^{M-1}}$$

The rate of loss of heat from the cylindrical surface of node M is

$$q'=h\times(T_M^i-T_f)$$

The rate of accumulation of heat between the nodes, M-1/2 and M per unit length is

$$q'=-k\times\frac{(T_1^i-T_0^i)}{\Delta r\times r^{M-1}}\times 2\times pi(R-\frac{\Delta r\times r^{M-1}}{2})\times 1$$
$$-h\times 2\times pi\times R\times 1(T_M^i-T_f)+S\times v$$

where, $v=pi\{\mathrm{R}^2-(R-\frac{\Delta r\times r^{M-1}}{2})^2\}\times 1=$
$$pi\{R\Delta r\times r^{M-1}-\frac{\Delta r^2\times r^{2M-2}}{4}\}$$

Applying energy balance

$$-k\times\frac{(T_1^i-T_0^i)}{\Delta r\times r^{M-1}}\times 2\times pi(R-\frac{\Delta r\times r^{M-1}}{2})\times 1$$
$$-h\times 2\times pi\times R\times 1(T_M^i-T_f)+S\times(pi\{\mathrm{R}^2-(R-\frac{\Delta r\times(r)^{M-1}}{2})^2\}\times 1)$$
$$=pi(R\Delta r\times r^{M-1}-\frac{\Delta r^2\times r^{2M-2}}{4})\times\rho c_p\times\frac{(T_M^{i+1}-T_M^i)}{\Delta t}$$

$$\frac{\Delta r\times r^{M-1}}{\Delta t}(R-\frac{\Delta r\times r^{M-1}}{4})\times\rho c_p T_M^{i+1}=\frac{2k}{\Delta r\times r^{M-1}}(R-\frac{4r\times r^{M-1}}{4})T_{M-1}^{i}$$
$$+\{\frac{\Delta r\times r^{M-1}}{\Delta t}(R-\frac{\Delta r\times r^{M-1}}{4})\times\rho c_p-\frac{2k}{\Delta r\times r^{M-1}}(R-\frac{\Delta r\times r^{M-1}}{4})$$
$$-2Rh\}T_M^i+2RhT_f+\Delta r\times r^{M-1}(R-\frac{\Delta r\times r^{M-1}}{4})S$$

Hence, the equation of the surface node M is;

Equation 8

$$T_M^{i+1}=\frac{2\alpha\Delta t}{(\Delta r\times(r)^{M-1})^2}\frac{(R-\frac{\Delta r\times(r)^{M-1}}{2})}{(R-\frac{\Delta r\times(r)^{M-1}}{4})}T_{m-1}^{i}$$
$$+\{1-\frac{2\alpha\Delta t}{(\Delta r\times(r)^{M-1})^2}\frac{(R-\frac{\Delta r\times(r)^{M-1}}{2})}{(R-\frac{\Delta r\times(r)^{M-1}}{4})}-\frac{2\alpha h\Delta tR}{K\Delta r\times \mathrm{r}^{M-1}}\frac{(R-\frac{\Delta r\times(r)^{M-1}}{2})}{(R-\frac{\Delta r\times(r)^{M-1}}{4})}\}T_m^i$$
$$+\frac{2\alpha h\Delta tR}{K\Delta r\times \mathrm{r}^{M-1}(\frac{\Delta r\times(r)^{M-1}}{4})}T_f+\frac{\alpha\Delta t}{k}S$$

Heat content of the wire

The temperature at various nodes can be calculated using the equations 6, 7, and 8. The heat content of the portion between m = 0 and m = ½ is:

Equation 9

$$=\{pi(\Delta r\times r^{m-1})^2\}\times l\times\rho\times C_p\times(\mathrm{T}_0)$$

The change in heat content between the portion m = M-1/2 and m = M is:

Equation 10

$$=\{piR^2-Pi(R-\frac{\Delta r\times r^{M-1}}{2})^2\}\times l\times\rho\times C_p\times(\mathrm{T}_M-T_a)$$
$$=\{piR\Delta r\times r^{M-1}-\frac{pi}{4}(\Delta r\times r^{M-1})^2\}l\times\rho\times C_p\times(\mathrm{T}_M-T_a)$$

The change in heat content of any portion between nodes m-1/2 and m+1/2 is :

Equation 11

$$=pi\{(R_m+\frac{\Delta r\times r^m}{2})^2-(R_m-\frac{\Delta r\times r^{m-1}}{2})^2\}\times l\times\rho\times C_p\times(\mathrm{T}_M-T_a)$$
$$=pi(\Delta r)^2 r^{m-1}(r+1)\{\frac{r^m-1}{r-1}+\frac{r^{m-1}(r-1)}{4}\}\times l\times\rho\times C_p\times(\mathrm{T}_M-T_a)$$

The total heat content of the cylindrical rod is:

Equation 12

$$\mathrm{pi}\,\Delta r l\rho C_p\{\frac{\Delta r}{4}(\mathrm{T}_0-T_a)+r^{M-1}(R-\frac{\Delta r\times r^{M-1}}{4})(\mathrm{T}_M-T_a)\}$$
$$+\mathrm{pi}(\Delta r)^2 l\rho C_p(r+1)\sum_{m=1}^{m=M-1}\{r^{m-1}(\frac{r^{m-1}}{r-1}+\frac{r^{m-1}(r-1)}{4})(\mathrm{T}_M-T_a)\}$$

Hence heat generated in the round (or the circumference of the wire) is given by:

Equation 13

$$=\{pir\Delta r\times r^{M-1}-\frac{pi}{4}(\Delta r\times r^{M-1})^2\times l\times S_{[\mathrm{M}]}+$$
$$\sum_{m=1}^{m=M-1}pi(\Delta r)^2 r^{m-1}(\mathrm{r}+1)(\frac{r^{m-1}}{r-1}+\frac{r^{m-1}(r-1)}{4})\times l\times S_{[\mathrm{M}]}$$
$$=\{pi\Delta r\times r^{M-1}(R-\frac{\Delta r\times r^{M-1}}{4})\times l\times S_{[\mathrm{M}]}+$$
$$pi(\Delta r)^2\times l(\mathrm{r}+1)\sum_{m=1}^{m=M-1}r^{m-1}(\frac{r^{m-1}}{r-1}+\frac{r^{m-1}(r-1)}{4})\times l\times S_{[\mathrm{M}]}$$

3. Initial calculation and boundary condition

Residence time of wire

The wire heating furnace was used to understand the heat transfer phenomena where an average temperature of 350 ^{O}C was maintained by rationalizing the control panel parameter of the induction heating machine as well as the line speed. A different line speed of the wire was maintained by adjusting the frequency of the spooler motor and the total residence time of the wire inside the furnace was calculated using the relation

T_{res} = length travelled (m) / line speed (m/s)

The residence time for various line speeds is tabulated in Table 1.

Table 1 Residence time of wire

Line speed	Res time
m/ min	s
25	1.04
33	0.79
41	0.64
49	0.53

Coil Efficiency: Power loss owing to water cooling of the copper coils

The copper coils, circular in shape, are provided with water jacket or channels so that they can be cooled efficiently and thus resulting in some power loss in the system. The loss of power owing to the water cooling of the copper coils was calculated as:

The flow rate of water = 15 liter/minute
Increase in cooling water temperature = 20 ^{O}C

Hence, Rate of heat loss = 15 [l/m] * 1 [kg/l] * 1[Cal/Kg ^{0}C] * 3 [^{0}C] = 45/60 [K Cal/s] = 30/60 * 4.1868 KJ/s = 2,09 KW
So, Coil Efficiency = $(12-2.09)/12$ = .825 or 82.5 %

Boundary conditions: Relevance of skin effect

Skin effect phenomena in the induction heating process occur when the current generates Ohmic losses, I^2R loss, is highest at the surface and diminishes exponentially toward the center and can be expressed as (Valery Rudnev, 2010)

Equation 14

$$I = I_0 e^{\frac{-x}{\delta}}$$

x = current at a depth x from the surface
I_0 =Current at surface (x= 0)
δ = depth of penetration at which the magnitude of the current drops to 0.368 of the surface current and hence called as skin depth. It can also be defined as the depth from the surface where 87% of the power consumption within the wire is taking place[3]]. The skin depth can be calculated using the relation given by (Edgar Rapoport, 2010) (S. Zinn, 1995)

Equation 15

$$\delta = \sqrt{\frac{\rho}{\pi \mu f}} = 0.3 \text{ mm}$$

Where,
ρ = resistivity of the strand wire (ohm.m) =0.16 * 10^{-6} ohm.m
μ = magnetic permeability of the load (H/m) = 4*Pi*10^{-5} H/m
f= frequency (Hz) = 4500 Hz

Hence 87% of the available power consumption inside the wire takes place at a depth of 0.3 mm from the surface and the rest 13% is consumed in between center and R - 0.3 mm, where R is the radius of the wire as shown in Figure 6. The available power or actual power dissipation distribution along the radius is given in Figure 7 for Φ 3.5 mm wire.

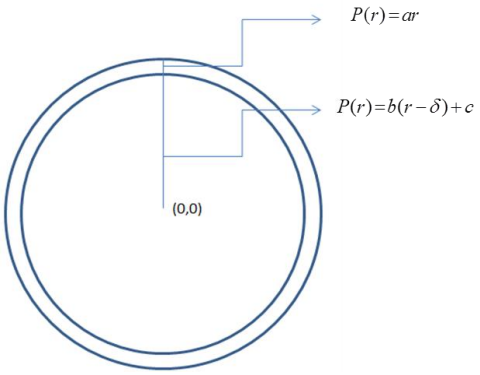

Figure 6 Power equation over the periphery of wire

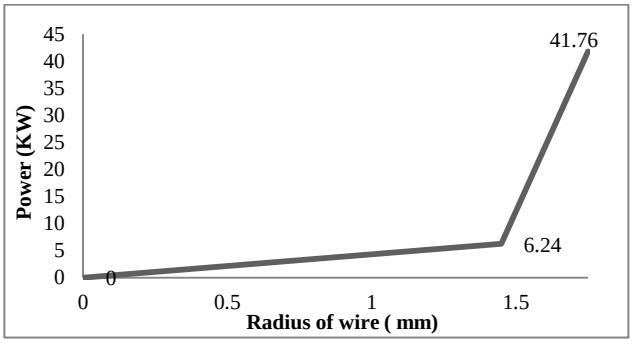

Figure 7 Distribution of power along the radius of 3.5 mm wire.

The power distribution equation can be written as
Equation 16

$$P_{[13\ \%\ of\ available\ Power]} = ar, \qquad 0 \le r < R - \delta,$$

$$P_{[87\ \%\ of\ available\ Power]} = br + c, \quad R - \delta \le r \le R,$$

Where P is power consumption in KW, R is radius in mm, δ is the skin depth and a, b, c are the constants.

4. Grid generation and numerical solution procedure

It is to be noted that initially the model was developed for uniform grid size where it had predicted a much lower value and the inaccuracy was due to very sharp change in the magnitude of the source term in the penetration depth zone. Hence, tuning of the model was done with variable grid size in geometric progression. A mathematical code was developed in C language where the equations 7 -16 were combined with the boundary condition given in equation 17. The simulation was run for 250 number of nodes with a time step of 0.00001 second. The material properties used are shown in Table 2.

Table 2 Material Properties for the cylindrical wire

Name	Value	Unit
Heat capacity at constant pressure	500	J/(kg*K)
Density	7800	Kg/m^3
Thermal conductivity	40	W/(m*K)

The temperature profile obtained for the residence time of 1.25 second for Φ 3.5 mm wire is shown in the Figure 8.

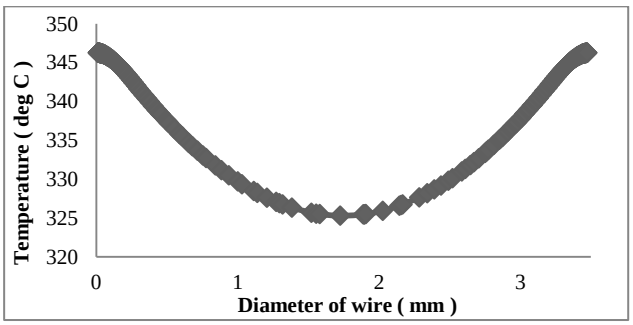

Figure 8 Variation of temperature of 3.5 mm wire with respect to diameter at residence time of 1.25 seconds

The temperature obtained at the center was 326 ^{O}C whereas the surface temperature was 346 ^{O}C. The temperature difference between the surface and the center was 20 ^{O}C.

5. Validation with plant trial

Trial experiments were conducted using 25 KVA wire heating machine as shown in Figure 9. Specific arrangement was made to run the wire continuously inside the furnace at a certain line speed using a spooler motor as discussed in Figure 1.

Figure 9 Induction Heating machine used for plant trial

The surface temperature of the wire was measured using a PK-27^{TM} SureGrip Industrial Surface Temperature Probe, a kind of type K thermocouples. The characteristics of the thermocouple are given in Table 3.

Table 3 Characteristics of thermocouple

Time constant	1 time constant equals 330 ms; 5 time constants equal final reading
Maximum Voltage Rating at Probe Tip	24 V AC rms, or 60 V DC
Probe Tip Max Temp	600 °C (1112 °F)
Probe Tip Material	303 stainless steel
Conductors	Type: K
Diameter:	22.9 mm (0.9 in)
Length	322.6 mm (12.75 in)

The speed of the spooler motor was adjusted in every step to achieve different line speeds of wire inside the furnace. The table 4 gives the surface temperature of the wire moving with a certain line speed inside the furnace and compared with the values obtained through the mathematical model.

The comparison plot in Figure 10 shows that the values predicted by the model matches closely with experimentally measured surface temperature.

Table 4 Plant trial versus the model prediction

Line speed		**Residence time**	**Surface Temperature**	
m/ min	**m/s**	**s**	**Experiment (^{o}C)**	**Model pred. (^{o}C)**
23	0.38	1.35	365	381.8
33	0.55	0.94	235	239.3
41	0.68	0.76	195	203.5
49	0.81	0.63	160	168.5

It is to be noted the value obtained from the model is somewhat higher than the experimental value because the measurement was taken just outside the furnace when the wire is coming out. There a small distance of 10 cm between the coil and the furnace outlet and therefore a drop of temperature due to natural convection is expected while measuring with the probe. The temperature profile of the wire along the diameter for various residence time periods, as indicated in Table 4, is shown in Figure 11.

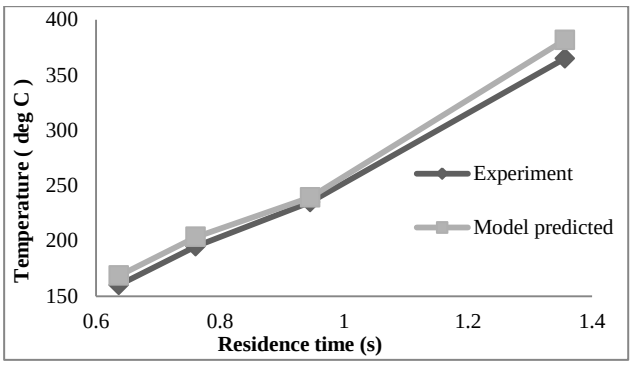

Figure 10 Comparison of model and experimental surface temperature of wire at different residence times

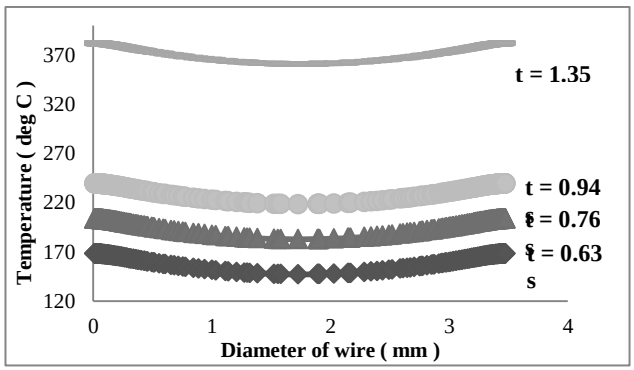

Figure 11 Variation of temperature with respect to diameter of wire at different residence time

The temperature difference between the center and the surface lie between 19 ^{O}C – 23 ^{O}C for all the four cases. It was observed that there exists a linear trend between the average temperature and time for each curve obtained. The plot of average temperature versus time for 3.5 mm wire is shown in Figure 12 and the best fit linear equation obtained was as follows:

T [^{O} C] = 299.79 * t [s] - 32.65

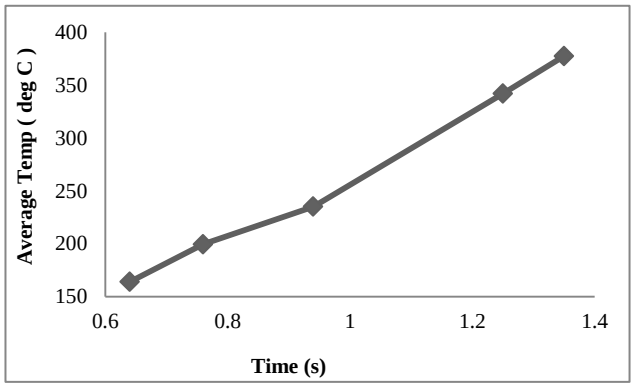

Figure 12 Variation of average temperature with respect to residence time for 3.5 mm wire

This can be helpful to extrapolate the average temperature that can be achieved for a particular residence time, or line speed, under the same operating condition. The equations 9-13 were used to generate the heat content of wire for different time steps as shown in the Figure 13. The difference between the center and surface was almost constant for all the residence time and it lies in the range of 9980 J/Kg - 10000 J/Kg.

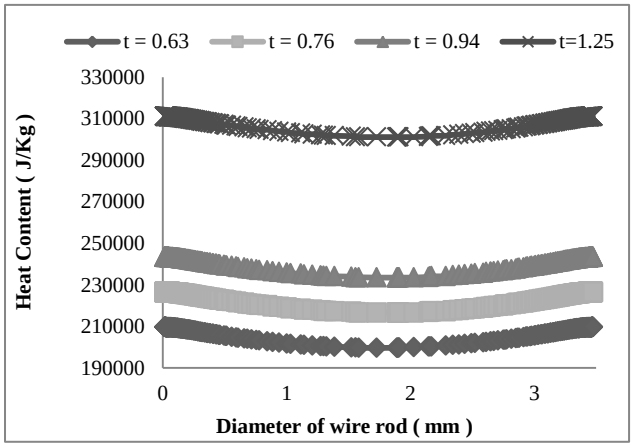

Figure 13 Heat content plot for different residence time

Tensile testing was performed in a tensile testing laboratory for the wire samples treated with various line speeds. It was found that uniform elongation increases with the surface temperature as shown in Figure 14. Evidently, the desired elongation range of 6% - 7% can be achieved if the line speed is maintained between 45 m/min – 50 m/min for the 3.5mm wire using the same wire heating machine.

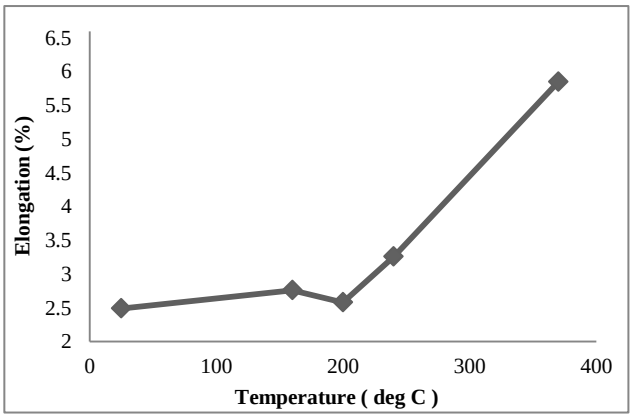

Figure 14 Plot for uniform elongation (%) versus the surface temperature

6. Summary and Conclusions

In the present work, the heat transfer during heating of a moving wire is expressed theoretically and validated experimentally in plant trial. A series of experiments were conducted on the wire heating machine and the reproducibility test were also performed to measure the thermal profile for various line speeds. The elongation obtained helped to ascertain that the difference in temperature between the center and the surface of Φ 3.5 mm wire is within the required range of 20 ^{0}C. A robust model is developed that can calculate constants in power boundary condition equations and the thermal profile for any wire diameter. The skin effect over the surface of cylindrical wire was applied in the form of heat source boundary condition at the surface which varies with the radius. The following conclusions were drawn from the study:

- Unsteady state simulation performed showed high surface temperature when residence time is low and it decreases with increase in line speed. The temperature difference between the center and the surface lies between 19^{O}C – 23 ^{0}C, which is required to achieve the desired mechanical properties. The heat content of the wire decreases with increase in line speed.
- Tensile testing helps to obtain the percentage elongation profile with temperature, which increases with more heating of wire due to decrease in line speed. The desired elongation range of 6% - 7% can be maintained if the line speed is maintained between 45 m/min – 50 m/min for the current wire heating machine.

References

Davies, E. (1990). Conduction and Induction Heating. London: Peter Peregrinus Ltd.

D. R. Poirier, G. H. (2012). Transport Phenomena in Materials Processing. John Wiley & Sons.

Edgar Rapoport, Y. P. (2010). Optimal Control of Induction Heating Process. Oxon, UK: Taylor and Francis Group.

S. Zinn, S. (1995). Elements of Induction Heating. ASM International.

Totten, G. E. (n.d.). Steel Heat Treatment - Equipment and Process Design. CRC Press.

Valery Rudnev, D. L. (2010). Handbook of Induction Heating. CRC press.

Nomenclature

T	Temperature
d	Wire diameter
r	Radius of wire
S	Source term
C_p	Specific heat
P_e	Peclet number
V	velocity of the moving wire
I	Current
Pi	constant, 3.14
f	Frequency
P	Power

Greek

K	Thermal conductivity
ρ	Density
μ	Magnetic permeability
α	Thermal diffusivity
δ	Depth of penetration

Subscripts

m	inside nodes
M	Surface node
i	Perpendicular component along the radius